Longitudinal Control of Heavy Trucks in Mixed Traffic: Environmental and Fuel Economy Considerations

Jianlong Zhang, *Member, IEEE*, and Petros A. Ioannou, *Fellow, IEEE*

***Abstract*—In this paper, longitudinal vehicle-following controllers for heavy trucks with different spacing policies are designed, analyzed, simulated, and experimentally tested, and their performance in mixed traffic with passenger vehicles is evaluated. A new vehicle-following controller for trucks, which has better properties than existing ones with respect to performance and impact on fuel economy and pollution during traffic disturbances, is developed. The response of trucks to disturbances caused by lead passenger vehicles is smooth due to the limited acceleration capabilities of trucks whether they are manual or equipped with adaptive cruise control (ACC) systems. Vehicles following the truck are therefore presented with a smoother speed trajectory to track. This filtering effect of trucks is shown to have beneficial effects on fuel economy and pollution. However, it creates large intervehicle gaps that invite cut-ins from neighboring lanes, creating additional disturbances. These cut-ins, under certain realistic scenarios, may reduce any benefits obtained by the smooth response of trucks as well as increase travel time. The results of this paper indicate possible benefits trucks may have in mixed traffic and also reinforces what is already known—that trucks could be detrimental to traffic flow.**

***Index Terms*—Adaptive control, automated highway systems, emission, fuel economy, vehicle automation.**

I. Introduction

IT IS ENVISIONED that automation is more likely to be introduced in heavy trucks than in passenger vehicles due to cost as well as human-factor considerations. Extensive studies have been done on adaptive cruise control (ACC), also referred to as intelligent cruise control (ICC). DaimlerChrysler has already developed automatic vehicle-following control systems for heavy trucks, referred to as an "electronic draw bar" system [1]. Others include the Eaton vehicle onboard radar (VORAD) collision avoidance system that allows a truck to perform automatic vehicle following maintaining a safe time headway in traffic [2]. At Partners for Advanced Transit and Highways (PATH), there have been several research efforts on truck automation [3]–[6]. The environmental performance of these automatic control systems as they begin to penetrate into the transportation system is very important. The expected positive effects, once validated by analysis and experiments, will help accelerate the deployment of automated heavy trucks as well as concepts of automated highway systems (AHS). It has been shown that the smooth response of ACC vehicles, designed for passenger comfort, significantly reduces fuel consumption and levels of pollutants during the presence of traffic disturbances [7], [8]. Studies on the potential impact of advanced public transportation systems (APTS) on air quality and fuel economy conclude that transit buses produce less hydrocarbon and carbon monoxide emissions than autos on a passenger-mile basis [9].

In this paper, we evaluate the performance of different vehicle-following controllers currently available for heavy trucks using microscopic simulations. Our simulation results indicate that the performance of a vehicle-following controller is mainly determined by the spacing policy employed rather than by its form. We therefore focused on proportional–integral–differential (PID) vehicle-following controllers for different spacing policies. A new vehicle-following controller is designed to provide better performance on the microscopic level with beneficial effects on fuel economy and pollution. The validated emission models for passenger vehicles and trucks developed in [10] and [11] are used to evaluate the impact of trucks on emissions and fuel economy. Experiments with actual vehicles are used to demonstrate the operation of the longitudinal controllers in real time and to validate our simulation models.

The sluggish dynamics of trucks, whether manual or ACC, due to limited acceleration capabilities make their response to disturbances caused by lead passenger vehicles smooth. Vehicles following the truck are therefore presented with a smoother speed trajectory to track. This filtering effect of trucks is shown to have beneficial effects on fuel economy and pollution. If the response of the truck is too sluggish, then a large intervehicle spacing may be created, inviting cut-ins from neighboring lanes. These cut-ins create additional disturbances with negative effects on fuel economy and emissions.

The paper is organized as follows. In Section II, the simulation models are presented. In Section III, we analyze a PID-type vehicle-following controller for different spacing policies and design a new vehicle-following controller. In Section IV, microscopic simulation results are used to demonstrate that the

Manuscript received July 30, 2004; revised May 25, 2005, July 21, 2005, and November 15, 2005. This work was supported by the California Department of Transportation through California Partners for Advanced Transit and Highways (PATH) of the University of California. The Associate Editor for this paper was B. K. Johnson.

The authors are with Center for Advanced Transportation Technologies, Department of Electrical Engineering—Systems, University of Southern California, Los Angeles, CA 90089 USA (e-mail: jianlong.zhang@usc.edu; ioannou@usc.edu).

Digital Object Identifier 10.1109/TITS.2006.869597

new controller can achieve better performance in the presence of traffic disturbances. In Section V, the simulation results are used to investigate the environmental performance of the new controller. In Section VI, experimental and simulation data are presented and used to validate the models used in the simulations. The conclusions are given in Section VII.

II. Vehicle Models

A. Longitudinal Dynamics of Heavy Trucks

In this study, the longitudinal truck model used for simulations is the same as in [3] and [4]. It is proposed in [5] and [6] and experimentally validated in Section VI. It can be characterized by a set of differential equations, algebraic relations, and look-up tables. The dominant state in this model is the one associated with the longitudinal speed v, which is determined by $\dot{v} = (F_{\rm t} - F_{\rm a} - F_{\rm r})/m$, where m is the vehicle mass, $F_{\rm t}$ is the tractive tire force, $F_{\rm a}$ is the aerodynamic drag force, and $F_{\rm r}$ is the rolling friction force. $F_{\rm a}$ is equal to $c_{\rm a}v^2$, where $c_{\rm a}$ is the aerodynamic drag coefficient, and $F_{\rm r}$ is equal to $c_{\rm r}mg/h_{\rm w}$, where $c_{\rm r}$ is the rolling friction coefficient, $h_{\rm w}$ is the radius of the front wheels, and g is the gravity constant. The brake/fuel commands are incorporated in the differential and algebraic equations that determine the tire force $F_{\rm t}$.

B. Human-Driver Model for Passenger Vehicles

Pipes' vehicle-following model [12] is chosen to simulate manually driven passenger vehicles, since it is found to be the most appropriate human-driver model for the type of simulations and experiments we perform in the sense that it models closely the vehicle-following behavior of the human driver in the presence of traffic disturbances [7]. Pipes' model is described as

$$a_i(t) = K\left[v_{i-1}(t-\tau) - v_i(t-\tau)\right] \tag{1}$$

where v_{i-1} and v_i are the speeds of the $i-1$th (leading the ith vehicle) and ith vehicles, respectively, a_i is the acceleration of the ith vehicle, K is the sensitivity factor, and τ is the reaction delay. In the simulations, we take $\tau = 1.5$ s and $K = 0.37\ \text{s}^{-1}$ [7].

C. Human-Driver Model for Heavy Trucks

In the human-driver model proposed by Bando *et al.* [13], the driver controls the acceleration in such a way that he/she maintains an optimal speed based on the following distance to the preceding vehicle. The human-driver model for heavy trucks used in our study is a modified version of Bando's model, which is expressed as (2), shown at the bottom of the page, where $\tau_{\rm t}$ is a time delay, $K_{\rm t}$ is the sensitivity factor for heavy trucks, x_{i-1} and x_i are the positions of the $i-1$th vehicle and the ith vehicle in a vehicle string, respectively, $A_{\min}$ and $A_{\max}$ are the lower and upper acceleration bounds, respectively, and $V(\cdot)$ is the desired speed as a function of the vehicle separation distance. We assume that the truck driver attempts to maintain a constant time headway during driving and the desired speed is set by $V(\Delta x_i) = \max\{0, (\Delta x_i - s_{\rm t0})/h_{\rm tm}\}$, where $\Delta x_i = x_{i-1} - x_i$ is the intervehicle spacing, $s_{\rm t0}$ is the spacing corresponding to the jam density, and $h_{\rm tm}$ is the time headway used by the truck driver. If there is no acceleration limit, $K_{\rm t}$ is infinitely large and the desired speed is not restricted to be nonnegative then the modified Bando's model is identical to Pipes' model. In the simulations, we take $K_{\rm t} = 0.8\ \text{s}^{-1}$, which is recommended in [14]. The time delay $\tau_{\rm t}$ is set as 1.0 s. It is shorter than the delay in Pipes' model since the truck driver sits high, views traffic far ahead, and is able to make decisions faster than the drivers in passenger vehicles who can usually view only the vehicle in front of them. The time headway $h_{\rm tm}$ is set as 3 s. It is larger than that used in Pipes' model for passenger vehicles since the truck has lower deceleration capability than passenger vehicles and truck drivers need to maintain longer headways for safety considerations. We use $s_{\rm t0} = 6.0$ m to account for the intervehicle spacing at zero or very low speeds. In our study, we consider that the human-driver model for heavy trucks describes the average behavior of human drivers.

III. Vehicle-Following Control Design

A. Control Objective and Constraints

In vehicle-following control, the ACC system regulates the vehicle speed v towards the speed of the lead vehicle $v_{\rm l}$ and keeps the intervehicle spacing $x_{\rm r}$ close to the desired spacing $s_{\rm d}$. With the time-headway policy, the desired spacing is given by $s_{\rm d} = s_0 + hv$, where s_0 is a fixed intervehicle spacing and h is the time headway. The control objective can be expressed as

$$v_{\rm r} \to 0,\ \delta \to 0 \qquad \text{as } t \to 0 \tag{3}$$

where $v_{\rm r} = v_{\rm l} - v$ is the relative speed and $\delta = x_{\rm r} - s_{\rm d}$ is the separation error. In the analysis, we assume that $v_{\rm l}$ and its derivative are continuous and bounded signals as this is the case in practice. There are two control constraints, as follows [15].

- C1) $a_{\min} \le \dot{v} \le a_{\max}$, where $a_{\min}$ and $a_{\max}$ are specified.
- C2) The absolute value of jerk $|\ddot{v}|$ should be small.

$$a_i(t) = \begin{cases} A_{\min}, & \text{if } K_{\rm t}\left(V\left(x_{i-1}(t-\tau_{\rm t}) - x_i(t-\tau_{\rm t})\right) - v_i(t)\right) < A_{\min} \\ A_{\max}, & \text{if } K_{\rm t}\left(V\left(x_{i-1}(t-\tau_{\rm t}) - x_i(t-\tau_{\rm t})\right) - v_i(t)\right) > A_{\max} \\ K_{\rm t}\left(V\left(x_{i-1}(t-\tau_{\rm t}) - x_i(t-\tau_{\rm t})\right) - v_i\right), & \text{otherwise} \end{cases} \tag{2}$$

The first constraint arises from the inability of the truck to generate high accelerations and from driver-comfort and safety considerations. The second one is for driver comfort.

B. Vehicle Model for Control Design

The longitudinal model used for control design is [15]

$$\dot{v} = -a(v - v_{\mathrm{d}}) + b(u - u_{\mathrm{d}}) + d \tag{4a}$$

$$v_{\mathrm{d}} = f_{\mathrm{u}}(u_{\mathrm{d}}) \tag{4b}$$

where v_{d} is the desired speed, u_{d} is the corresponding fuel command, d is the modeling uncertainty, a and b are unknown positive constant parameters that depend on the operating point, and f_{u} is a known smooth function of 1-1 mapping. In the following analysis, we assume that d and $\dot{d}$ are bounded. In the vehicle-following mode, the desired speed is the speed of the lead vehicle. Hence, the vehicle model for control design is described by (4a) and (4b) with $v_{\mathrm{d}} = v_{\mathrm{l}}$.

Remark 1: The model given by (4a) and (4b) is only used for control design while the nonlinear model introduced in Section II-A is used for simulations and experimental validation. a and b are unknown parameters since they change when gears are shifted or other variables change.

Remark 2: For control design and analysis, we assume that the relationship between v_{d} and u_{d} is described by a smooth function f_{u}. It may be argued that the relationship cannot be described by a smooth function in the practical situation since gear shifting and driving conditions will affect this relationship. However, the discrepancy between v_{d} and $f_{\mathrm{u}}(u_{\mathrm{d}})$ can be merged into the model uncertainty term d.

C. Control Design

In most studies on vehicle-following control such as that in [15], the time headway is chosen as a positive constant. A number of vehicle-following controllers can be designed based on the simplified vehicle model, and simulations or experiments demonstrate that they all work well when the control parameters are properly chosen [3], [4], [15]. In this paper, we use a PID-type controller

$$u = k_p(v_{\mathrm{r}} + k\delta) + k_i \frac{1}{s}(v_{\mathrm{r}} + k\delta) + k_{\mathrm{d}} \frac{s}{\frac{1}{N}s + 1}(v_{\mathrm{r}} + k\delta) \tag{5}$$

where s is the Laplace operator, and k, k_p, k_i, k_{d}, and N are positive control parameters to be chosen. With linear control analysis, it can be shown that the closed-loop system is stable if the control parameters are chosen so that $[a + bk_p(1 + kh)] \cdot [k_i(1 + kh) + kk_p] + bk^2k_{\mathrm{d}}k_p - kk_i > 0$ and N is sufficiently large [16]. Furthermore, v_{r} and δ converge exponentially fast to the residual set

$$E = \left\{ v_{\mathrm{r}} \in R, \delta \in R \,\middle|\, |v_{\mathrm{r}}| \le C_1 \cdot \|\dot{v}_{\mathrm{l}}(t)\|_\infty + C_2 \cdot \left\|\dot{d}(t)\right\|_\infty \right. \\ \left. \text{and} \quad |\delta| \le C_3 \cdot \|\dot{v}_{\mathrm{l}}(t)\|_\infty + C_4 \cdot \left\|\dot{d}(t)\right\|_\infty \right\} \tag{6}$$

for some finite constants $C_i > 0 (i = 1, \ldots, 4)$. v_{r} and δ converge to 0 exponentially fast if v_{l} and d are constants.

Using (6), the fuel command is issued when u is positive, while the brake is activated when $u < -u_0$ (u_0 is a positive design parameter). Otherwise, the brake system is inactive and the fuel system is operating as in idle speed. This is a simple switch logic that prevents frequent chattering between the two systems. This switch logic is based on the control effort u instead of the desired acceleration. A different switching logic can be found in [17].

The above analysis is for the case that h and k are both constants. In [18], the desired intervehicle spacing is set as

$$s_{\mathrm{d}} = s_0 + h_1 v + h_2 v^2 \tag{7}$$

where h_1 and h_2 are positive constants. We refer to (7) as the quadratic spacing policy. The time headway used in this policy is $h_1 + h_2 v$. In [4], the time headway h and the control parameter k are chosen as

$$h = \mathrm{sat}(h_0 - c_h v_{\mathrm{r}}), \; k = c_k + (k_0 - c_k)\exp(-\sigma\delta^2) \tag{8}$$

where h_0, c_h, k_0, c_k, and σ are positive constants to be designed (with $c_k < k_0$) and the saturation function $\mathrm{sat}(\cdot)$ has an upper bound 1 and a lower bound 0. Other choices of spacing rules based on traffic flow characteristics can be found in [19]. If the lead vehicle operates around a nominal speed $v_{\mathrm{l}0}$ and the vehicle-following controller efficiently keeps v_{r} and δ close to 0, the stability analysis for the constant-time-headway policy can be applied to the quadratic spacing policy and the nonlinear spacing policy in (8) for small perturbations around the nominal speed $v_{\mathrm{l}0}$.

To guarantee that the constraints C1) and C2) are not violated, we should avoid the generation of high or fast varying control signals. Such high or fast varying control signals can be generated by the control law (5) if the lead vehicle accelerates rapidly or changes lanes, creating a large spacing error, or the truck switches to a new target with large initial spacing error. In [3] and [4], these practical situations have not all been addressed since the emphasis was on truck platoon. In [15], a nonlinear filter is used to smooth the speed trajectory of the lead vehicle, and $\mathrm{sat}(\delta)$ is used instead of δ. These modifications work well for the passenger-vehicle case. However, in the heavy-truck case, fast varying v_{l} may also lead to fast varying δ since the heavy truck can only accelerate slowly, which indicates that δ should also be smoothed before being passed into the control system. Furthermore, in this case, the temporary separation error could be very large. If we simply use $\mathrm{sat}(\delta)$ for the controller (5), any changes in v_{l} will directly affect the control signal when $\delta > \mathrm{sat}(\delta)$, even if some changes in v_{l} should be ignored. In the following section, we design a new vehicle-following controller to address these issues in addition to others.

D. New Vehicle-Following Controller

Let us define $H \triangleq (\partial/\partial v)s_{\mathrm{d}}(v, v_{\mathrm{l}})$ and $H_{\mathrm{l}} \triangleq (\partial/\partial v_{\mathrm{l}})s_{\mathrm{d}}(v, v_{\mathrm{l}})$. Most choices of desired intervehicle spacing share the same property that $H \ge 0$ and H_{l} is bounded [4], [15], [18], [19]. For the constant-time-headway rule, H is equal to the

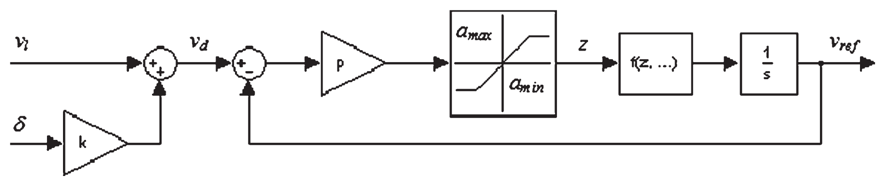

Fig. 1. Nonlinear filter used in the new vehicle-following controller.

time headway h, and H_{l} is 0. In the following analysis, we always assume that H and H_{l} are bounded since in practice, it is impossible to employ time headways involving arbitrarily large H and H_{l}.

Lemma 1: For the vehicle-following problem described in Section III-A, if the controller is designed such that $(v_{\mathrm{r}} + k\delta) \to 0$ (k is a positive constant) as $t \to \infty$ and $d/dt\,(v_{\mathrm{r}} + k\delta)$ is uniformly continuous, then v_{r} and δ are bounded. In addition, if v_{l} is a constant, then the control objective in (3) is achieved.

Proof: If $(d/dt)(v_{\mathrm{r}} + k\delta)$ is uniformly continuous and $(v_{\mathrm{r}} + k\delta) \to 0$ as $t \to \infty$, then it follows from Barbalat's Lemma [20] that $(d/dt)(v_{\mathrm{r}} + k\delta) \to 0$ as $t \to \infty$, and therefore

$$\frac{d}{dt}(v_{\mathrm{r}} + k\delta) = (1 + kH)\dot{v}_{\mathrm{r}} + kv_{\mathrm{r}} - k(H + H_{\mathrm{l}})\dot{v}_{\mathrm{l}} \to 0 \quad (9)$$

as $t \to \infty$. It also follows from $(d/dt)(v_{\mathrm{r}} + k\delta)$ being uniformly continuous and $(d/dt)(v_{\mathrm{r}} + k\delta) \to 0$ as $t \to \infty$ that $(d/dt)(v_{\mathrm{r}} + k\delta)$ is bounded. Since k is a positive constant, $H > 0$, and H, H_{l}, and $\dot{v}_{\mathrm{l}}$ are bounded, it follows that v_{r} is bounded. In addition, $(v_{\mathrm{r}} + k\delta)$ is uniformly continuous since $(d/dt)(v_{\mathrm{r}} + k\delta)$ is bounded. Hence, it can be shown that $(v_{\mathrm{r}} + k\delta)$ is bounded since it is uniformly continuous and converges to 0. Hence, δ is bounded. In particular, if v_{l} is a constant, then (9) implies $v_{\mathrm{r}} \to 0$, and therefore $\delta \to 0$. ■

Lemma 1 indicates that the vehicle-following task can be viewed as a special speed tracking task, in which the desired speed v_{d} is equal to $v_{\mathrm{l}} + k\delta$. If we design the vehicle-following controller such that $v \to v_{\mathrm{l}} + k\delta$ in a proper way, then v_{r} and δ are guaranteed to be bounded, and the control objective in (3) can be achieved when v_{l} is a constant.

We propose a speed tracking controller as

$$u = f_{\mathrm{u}}^{-1}(v_{\mathrm{d}}) + k_1 e_v + k_2 + k_3 \dot{v}_{\mathrm{d}} \quad (10)$$

where $e_v = v_{\mathrm{d}} - v$, and the control parameters $k_i (i = 1, 2, 3)$ are updated by

$$\dot{k}_1 = \mathrm{Proj}\left\{\gamma_1 e_v^2\right\},\ \dot{k}_2 = \mathrm{Proj}\{\gamma_2 e_v\},\ \dot{k}_3 = \mathrm{Proj}\{\gamma_3 e_v \dot{v}_{\mathrm{d}}\}. \quad (11)$$

In (11), $\gamma_i (i = 1, 2, 3)$ are positive design parameters, and $\mathrm{Proj}\{\cdot\}$ is the projection function limiting k_i between their lower bounds $k_{\mathrm{l}i}$ and upper bounds $k_{\mathrm{u}i} (i = 1, 2, 3)$.

Lemma 2: Consider the system represented in (4a) and (4b) with the adaptive speed tracking controller in (10) and (11). If $k_{\mathrm{l}i}$ and $k_{\mathrm{u}i} (i = 1, 2, 3)$ are properly chosen, then all the closed-loop signals are bounded. In addition, the following conditions are derived.

1) If d is a constant, then $e_v \to 0$ as $t \to \infty$.
2) If d is a constant and $\dot{v}_{\mathrm{d}}$ is uniformly continuous, then e_v, $\dot{e}_v \to 0$ as $t \to \infty$.

Proof: For the system represented in (4a) and(4b), if a, b, and d are known, then we can apply the controller

$$u = f_{\mathrm{u}}^{-1}(v_{\mathrm{d}}) + k_1^* e_v + k_2^* + k_3^* \dot{v}_{\mathrm{d}} \quad (12)$$

where $k_1^* = (a_m - a)/b$, $k_2^* = -d/b$, $k_3^* = 1/b$, and a_m is a positive constant. The close-loop system is $\dot{e}_v = -a_m e_v$. Hence, e_v, $\dot{e}_v \to 0$ as $t \to \infty$. Since a, b, and d are unknown, the control law (10) is proposed, and the closed-loop system can be rewritten as

$$\dot{e}_v = -a_m e_v - \widetilde{k}_1 e_v - \widetilde{k}_2 - \widetilde{k}_3 \dot{v}_{\mathrm{d}} \quad (13)$$

where $\tilde{k}_i = k_i - k_i^*$, $(i = 1, 2, 3)$. Consider the following Lyapunov function:

$$V = \frac{e_v^2}{2} + \frac{b\widetilde{k}_1^2}{2\gamma_1} + \frac{b\widetilde{k}_2^2}{2\gamma_2} + \frac{b\widetilde{k}_3^2}{2\gamma_3}. \quad (14)$$

If $k_{\mathrm{l}i}$ and $k_{\mathrm{u}i}$ are chosen such that $k_{\mathrm{l}i} \le k_i^* \le k_{\mathrm{u}i}$ for each i, then with the update law in (11), it can be derived that

$$\dot{V} = e_v \dot{e}_v + \frac{b}{\gamma_1}\tilde{k}_1 \dot{\tilde{k}}_1 + \frac{b}{\gamma_2}\tilde{k}_2 \dot{\tilde{k}}_2 + \frac{b}{\gamma_3}\tilde{k}_3 \dot{\tilde{k}}_3 \le -a_m e_v^2 + \frac{1}{\gamma_2}\tilde{k}_2 \dot{d}. \quad (15)$$

It can be shown [20] that all the signals inside the closed loop are bounded. Equation (15) also implies that if d is a constant, then $e_v \in L_2 \cap L_\infty$ and $\dot{e}_v \in L_\infty$, which means $e_v \to 0$. Furthermore, if $\dot{v}_{\mathrm{d}}$ is uniformly continuous, the $\dot{e}_v$ is also uniformly continuous. Using Barbalat's Lemma, we can show that $\dot{e}_v$ converges to zero as t goes to infinity. ■

Since the selected desired speed $v_{\mathrm{l}} + k\delta$ may vary fast, we employ the nonlinear filter in Fig. 1 to generate a smooth signal v_{ref} to be tracked. The saturation function inside the nonlinear filter serves as an acceleration limiter that restricts the change rate of v_{ref} between $a_{\min}$ and $a_{\max}$. The signal generated by the acceleration limiter is $z = \mathrm{sat}\{p(v_{\mathrm{l}} + k\delta - v_{\mathrm{ref}})\}$, where p is a positive design parameter. The function after the acceleration limiter is designed to accept or ignore the change rate signal z, and is given as (16), shown at the bottom of the next page, where m_v and M_v are constant design parameters with $0 < m_v < M_v$. The purpose of this nonlinear filter is to limit the change rate of v_{ref} between $a_{\min}$ and $a_{\max}$ and prevent v_{ref} from becoming much higher or lower than v_{l}. By regulating the truck's speed towards v_{ref}, the ACC system forces the truck to follow the preceding vehicle in a safe and comfortable way, while meeting the control objective (3).

Remark 3: Even though the signal z within the nonlinear filter in Fig. 1 is continuous, the function (16) may generate discontinuous signals that may cause problems in the analysis related to the existence and uniqueness of solutions of the resulting differential equation. The discontinuities may arise when $v_{\rm ref}$ varies around $v_{\rm l} - m_v$, $v_{\rm l} + m_v$, or $v_{\rm l} + M_v$. However, the function (16) can be slightly modified so that it will always generate continuous signals when z is continuous. For example, we can choose a small positive constant ε, and when $z > 0$ and $v_{\rm l} + m_v - \varepsilon \leq v_{\rm ref} < v_{\rm l} < m_v$ are satisfied, we set f equal to $(v_{\rm l} + m_v - v_{\rm ref}) \cdot z/\varepsilon$ instead of z. This minor modification will guarantee that no discontinuous signals are generated when $v_{\rm ref}$ varies around $v_{\rm l} + m_v$.

Lemma 3: Consider the system in (4a) and (4b) with the controller given as in (10) and (11) with $v_{\rm d}$ replaced by $v_{\rm ref}$. If $k_{{\rm l}i}$ and $k_{{\rm u}i} (i = 1, 2, 3)$ are properly chosen and $v_{\rm ref}$ is generated by the filter in Fig. 1, then u, v, and $v_{\rm r}$ are bounded. In addition, the following conditions are derived.

1) If d is a constant, then $v \to v_{\rm ref}$ and $\dot{v} \to \dot{v}_{\rm ref}$ as $t \to \infty$.
2) If $v_{\rm l}$ and d are constants, and the control parameters are chosen such that

$$\left(\frac{1}{k} + \inf H\right) |a_{\min}| > m_v, \ \left(\frac{1}{k} + \inf H\right) a_{\max} > m_v \quad (17)$$

where inf H is the infimum of H, then all the signals are bounded. ■

Due to the limited space, the proof for Lemma 3 is omitted and it can be found in [21]. The simulation results demonstrate that the control objective (3) can be achieved when $v_{\rm l}$ is a constant, even though we have not proven it.

In summary, the new ACC system is formed by the reference speed generator in Fig. 1 and the speed tracking controller given in (10) and (11), with $v_{\rm d}$ replaced with $v_{\rm ref}$. As demonstrated by the simulation results in Section IV, the new ACC system can effectively attenuate certain speed disturbances in mixed traffic situations. It can also prevent the actuator saturation problem for heavy trucks [21]. In [22], Bae and Gerdes have used a different technique called "input shaping" to prevent actuator saturation and improve vehicle-following performance for truck platooning.

In addition to the nonlinear shaping function of the reference speed, the following switching rules are incorporated in the new ACC system:

S1) If the separation distance $x_{\rm r}$ is larger than $x_{\max}$ ($x_{\max}$ is a positive design constant), then the fuel system is on.

S2) If the separation distance $x_{\rm r}$ is smaller than $x_{\min}$ ($x_{\min}$ is a positive design constant), then the brake system is on.

S3) $x_{\min} \leq x_{\rm r} \leq x_{\max}$, then the fuel system is on when $u > 0$, while the brake is activated when $u < -u_0$. When $-u_0 \leq u \leq 0$, the brake system is inactive and the fuel system is operating as in idle speed.

Switching rules S1) and S2) in the vehicle-following mode are used to avoid unnecessary activities of the brake or fuel systems when the vehicle separation is large or small enough.

IV. Simulation Studies

Simulations are carried out using Matlab/Simulink to investigate how different trucks would affect the speed and separation responses of the following passenger vehicles. The dynamics of the ACC trucks are modeled using the validated nonlinear model proposed in [5] and [6], the human drivers for passenger cars are modeled using Pipes' model, and the drivers for trucks are modeled using the modified Bando's model. For easy reference, we use ACC_N, ACC_Q, ACC_C, and ACC_NEW to represent automated trucks with the nonlinear spacing rule in (8), quadratic spacing rule, constant-time-headway rule, and the newly developed controller, respectively. We use M_PV and M_T to represent manually driven passenger vehicles and trucks, respectively.

We simulate and compare six vehicle strings, each containing ten vehicles. The lead vehicles in the six strings generate the same speed trajectory to be followed by the vehicles in the string. The second vehicles in the six strings are M_PV, M_T, ACC_N, ACC_Q, ACC_C, and ACC_NEW, respectively. The other eight vehicles in each string are manually driven passenger vehicles following the second vehicle. The parameters for the ACC systems are chosen as follows:

1) ACC_N: $h_0 = 1.6$, $k_0 = 1$, $c_h = 0.2$, $c_k = 0.5$, $\sigma = 0.1$, and $s_0 = 6.0$ m;
2) ACC_Q: $h_1 = 0.8$, $h_2 = 0.03$, $k = 0.2$, and $s_0 = 6.0$ m;
3) ACC_C: $h = 1.6$, $k = 0.2$, and $s_0 = 6.0$ m;
4) ACC_NEW: $h = 1.6$, $k = 0.2$, $s_0 = 6.0$ m, $p = 10$, $m_v = 2.0$ m/s, $M_v = 8.0$ m/s, and $a_{\min}$ and $a_{\max}$ used for the nonlinear filter in Fig. 1 are chosen based on the capabilities of the truck and desired driver-comfort considerations.

In the simulations, the truck weight is fixed at 20 T. In ACC_N, ACC_Q, and ACC_C, the speed of the lead vehicle is processed with the nonlinear filter used in [15]. We also use $\mathrm{sat}(\delta)$ in ACC_Q and ACC_C to eliminate the adverse effect of large separation errors. The PID parameters for the ACC systems are tuned for each truck to achieve good vehicle-following

$$f(z, v_{\rm ref}, v_{\rm l}) = \begin{cases} z, & \text{if } v_{\rm l} + m_v \leq v_{\rm ref} \leq v_{\rm l} + M_v \text{ and } z < 0 \text{ or } v_{\rm l} - m_v < v_{\rm ref} < v_{\rm l} + m_v \text{ or } v_{\rm ref} \leq v_{\rm l} - m_v \text{ and } z > 0 \\ 0, & \text{if } v_{\rm l} + m_v \leq v_{\rm ref} \leq v_{\rm l} + M_v \text{ and } z \geq 0 \text{ or } v_{\rm ref} \leq v_{\rm l} - m_v \text{ and } z \leq 0 \\ a_{\min}, & \text{if } v_{\rm ref} > v_{\rm l} + M_v \end{cases} \quad (16)$$

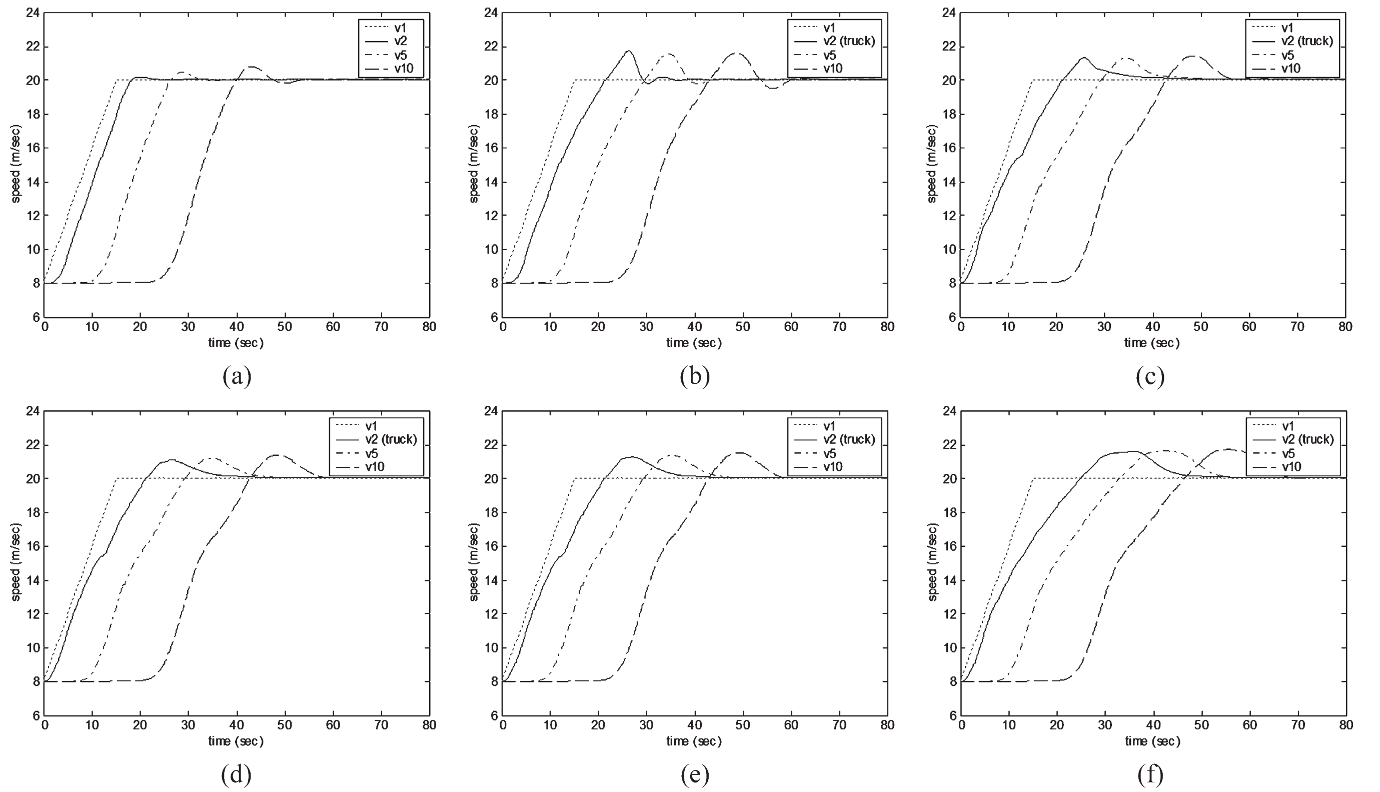

Fig. 2. Low-acceleration maneuvers: Speed responses of the six vehicle strings [(a)–(f) correspond to strings 1–6, respectively].

performance. It should be noticed that we cannot avoid actuator saturation by simply decreasing the PID gains for ACC_N, ACC_Q, and ACC_C since small gains will deteriorate the vehicle-following performance due to the slinky effect.

In our simulations, we assume that the ranging sensor installed on ACC trucks to measure intervehicle distance and relative speed has a maximum operation range of 120 m. If the vehicle separation distance is larger than 120 m, the ACC system will switch from the vehicle-following mode to the speed tracking (self-cruising) mode.

A. Low-Acceleration Maneuvers

In these simulations, the lead passenger vehicle accelerates from 8 to 20 m/s with a constant acceleration of 0.8 m/s^2, and then cruises at a constant speed. The 0.8-m/s^2 acceleration is easily achievable by the passenger vehicles but it is larger than the maximum acceleration a heavy truck could achieve with the particular trailer mass used in the simulations. Fig. 2 shows the speed responses of the six vehicle strings. The response labeled by "vi" corresponds to the ith vehicle in one vehicle string. It is indicated that the manually driven truck behavior is similar to that of the second passenger vehicle in vehicle string 1. The truck, however, has to reach its maximum acceleration limit in order to follow the preceding vehicle, leading to a slightly larger overshot in the speed response.

The speed responses of the four ACC trucks are similar, and they are all smoother than that of the manually driven truck. It is also shown in Fig. 2 that using ACC systems can significantly reduce the time delay in the speed response caused by the human driver. The controllers in ACC_N, ACC_Q, and ACC_C tend to generate large control efforts in the presence of large relative speeds and separation errors, which easily leads to fuel system saturation. However, the newly developed ACC controller regulates the truck's speed towards a smooth reference speed generated by the nonlinear filter in Fig. 1. Therefore, its fuel system responds in a smooth way and the fuel saturation is avoided. The truck's acceleration is kept within the desired acceleration limits $a_{\min}$ and $a_{\max}$. Due to the limited space, the responses of fuel commands are not presented here and they can be found in [21].

B. High-Acceleration Maneuvers

In this case, the lead vehicle accelerates from 8 to 20 m/s with a constant acceleration of 2 m/s^2 and then cruises at a constant speed. The speed responses of the six vehicle strings are presented in Fig. 3.

Compared with the manual passenger car, the separation error for the manual truck is temporarily larger due to its inability to accelerate as fast as the lead passenger vehicle. The truck driver has to regulate the vehicle speed much higher than that of the lead vehicle in order to close in and maintain the desired spacing. This leads to a peak in the speed response, as shown in Fig. 3(b), which indicates that the slinky effect of a manually driven heavy truck is more serious than that of a passenger vehicle. Fig. 3(c)–(f) shows the speed responses in vehicle strings 3–6, respectively. The vehicle-following controller used in ACC_N is most aggressive due the nonlinear spacing policy. The new ACC controller regulates the truck's speed in a smooth way without having to saturate the fuel system, while

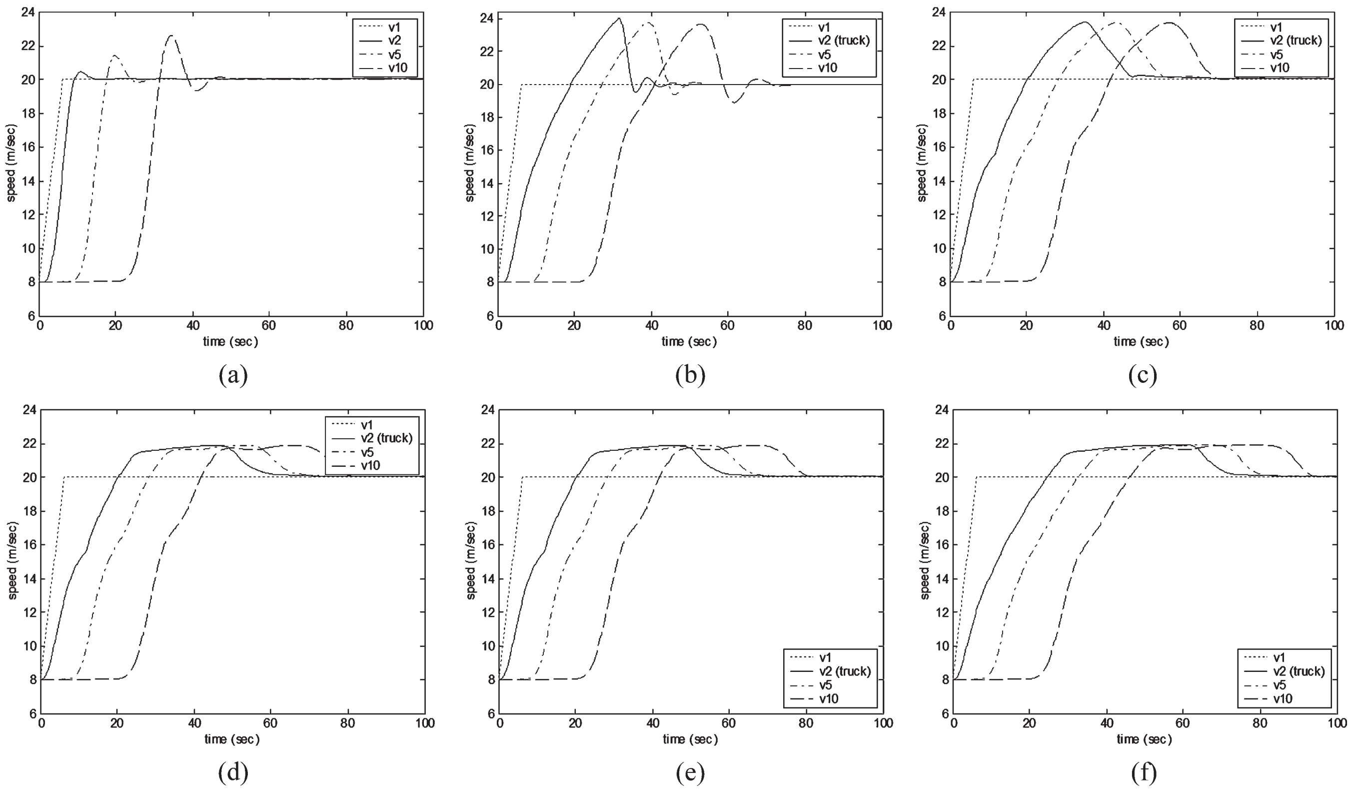

Fig. 3. High-acceleration maneuvers: Speed responses of the six vehicle strings [(a)–(f) correspond to strings 1–6, respectively].

all the other ACC systems saturate the fuel systems. Detailed information can be found in [21].

C. High-Acceleration Maneuvers With Oscillations

In this case, we simulate the situation where the lead passenger vehicle accelerates from 8 to 16 m/s with a constant acceleration of 2.0 m/s^2, and its speed oscillates around 16 m/s before settling to the constant speed of 16 m/s. This situation may arise in today's traffic where traffic disturbances downstream create a situation where the driver speeds up and then slows down in an oscillatory fashion before reaching steady state. The speed oscillations may also arise due to lane-change behaviors before the lead vehicle. In this situation, the temporary separation distance between the first and second vehicles will be very large, and we would like to investigate how the vehicles in the various strings of vehicles considered will behave with respect to the speed oscillations of the lead vehicle.

Fig. 4 shows the speed responses in the six vehicle strings. The speed disturbance introduced by the lead vehicle is transferred upstream unattenuated due to the aggressive behavior of human drivers, as shown in Fig. 4(a) and (b). Among all the ACC trucks, ACC_N is the most aggressive, and behaves similarly to the manually driven truck. Though ACC_C and ACC_Q perform better than ACC_N, when their speeds exceed that the lead vehicle, the speed disturbance is transferred upstream unattenuated. This is due to the use of $\mathrm{sat}(\delta)$. The control effort generated by (5) will be directly affected by v_1, since $\mathrm{sat}(\delta)$ is always a constant when δ is large. The new ACC system, however, can efficiently attenuate the speed disturbance in this situation, as shown in Fig. 3(f). This attenuation is due to the use of the nonlinear filter in Fig. 1. However, the speed disturbance can only be attenuated when the separation error is positive. When the separation error is negative, the ACC truck's response will be to reduce the separation error for safety reasons rather than reduce the oscillations.

V. Fuel Economy and Emissions

In this section, we investigate how different heavy trucks affect the fuel economy and emissions of the following passenger vehicles in the presence of different traffic disturbances simulated Section IV. We also investigate how different ACC systems affect the fuel efficiency and emissions of the heavy trucks. In addition, we investigate how the new proposed ACC system affects the following vehicles in the presence of speed limits or cut-in vehicles.

In the emission analysis, the quantities measured are the tailpipe emissions of unburned hydrocarbons (HC), monoxide of carbon (CO), oxides of nitrogen (NO, NO_2, denoted by NO_x) and fuel consumption. For passenger vehicles, the comprehensive modal emissions model (CMEM) developed at the University of California (UC), Riverside, is used to calculate the air pollution and fuel consumption [11]. The emission prediction model used for heavy trucks is developed by the same research group [10]. The inputs for the two models are vehicle speed and acceleration, while road grade is taken as 0 and no wind gust is considered. The outputs generated by the two emission models include tailpipe emissions of HC, CO, and NO_x, and fuel consumption.

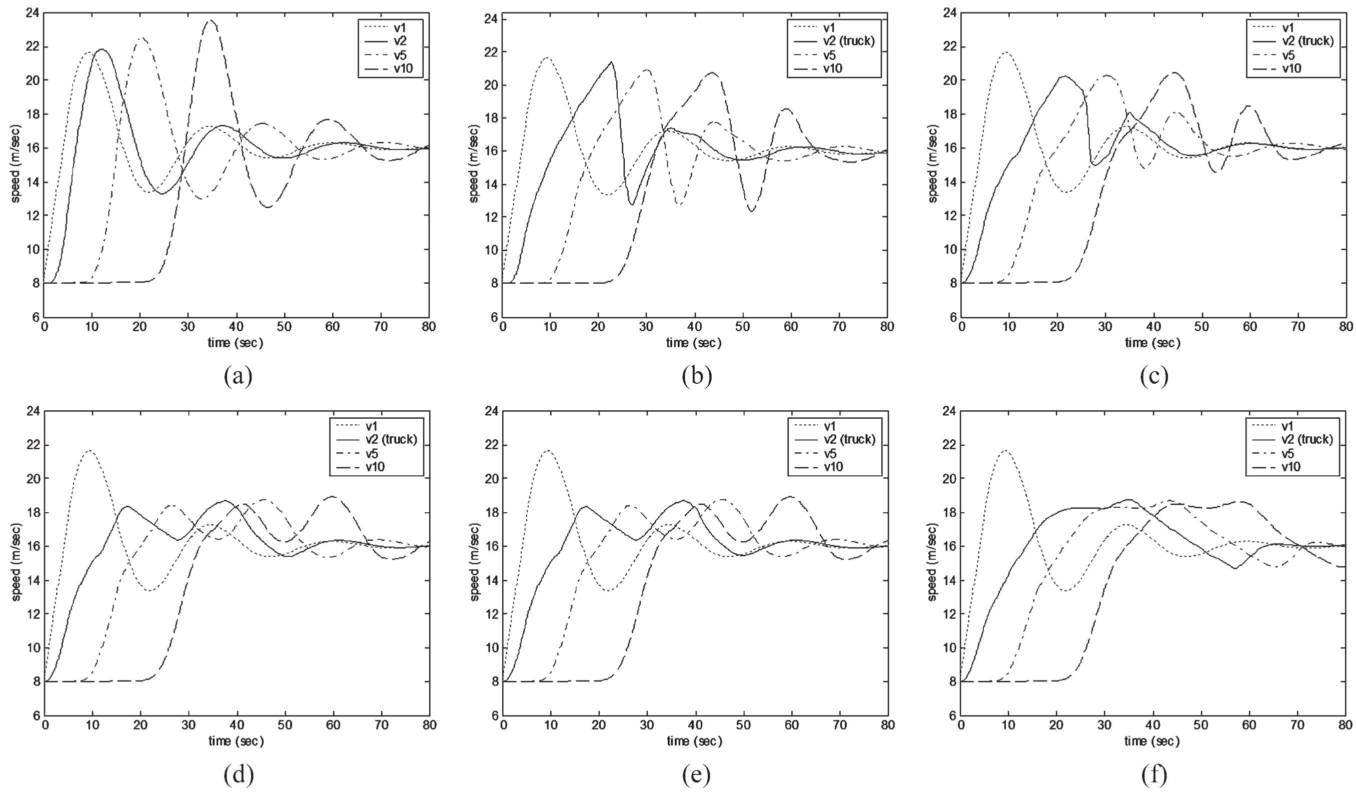

Fig. 4. High-acceleration with oscillations: Speed responses of the six vehicle strings [(a)–(f) correspond to strings 1–6, respectively].

TABLE I
TRAVEL TIME, FUEL, AND EMISSION BENEFITS OF THE EIGHT PASSENGER VEHICLES FOLLOWING THE TRUCK IN A STRING OF TEN VEHICLES FOR LOW-ACCELERATION MANEUVERS OF THE LEAD VEHICLE (NO CUT-INS)

Vehicle String (with)	1 (M_PV)	2 (M_T)	3 (ACC_N)	4 (ACC_Q)	5 (ACC_C)	6 (ACC_NEW)
Travel Time(sec)	73.7	73.9	73.3	73.2	73.3	73.3
Fuel (g)	0% (618)	≈ 0	≈ 0	≈ 0	≈ 0	4.3%
CO (g)	0% (20.6)	≈ 0	7.3%	6.4%	6.0%	9.4%
HC (g)	0% (0.93)	≈ 0	7.1%	6.3%	5.9%	9.2%
NO_x (g)	0% (1.51)	9.1%	10.0%	12.1%	10.7%	24.5%

TABLE II
FUEL AND EMISSION BENEFITS OF THE HEAVY TRUCK DURING LOW-ACCELERATION MANEUVERS OF THE LEAD VEHICLE (NO CUT-INS)

	M_T	ACC_N	ACC_Q	ACC_C	ACC_NEW
Fuel (g)	0% (594.8)	5.8%	6.0%	5.4%	6.6%
CO (g)	0% (5.27)	5.3%	5.3%	5.1%	6.2%
HC (g)	0% (0.26)	≈ 0	≈ 0	≈ 0	≈ 0
NO_x (g)	0% (12.42)	4.8%	4.8%	4.2%	5.8%

A. Low-Acceleration Maneuvers

In this case, the lead passenger vehicle accelerates from 8 to 20 m/s with a constant acceleration of 0.8 m/s^2 and then cruises at a constant speed. We calculate the fuel consumption and emissions of each vehicle from the time the lead vehicle begins to accelerate, until the string covers a distance of 1.2 km, as this is the distance taken by the vehicles to reach a steady-state speed after completing the acceleration maneuver. The travel time is also recorded over a distance of 1.2 km.

Table I shows the travel times and fuel and emission benefits for the last eight passenger vehicles in each vehicle string in the presence of a different truck in the second position in the string of the ten vehicles. The data in the second column are for vehicle string 1 (all manually driven passenger vehicles), and the fuel and emission benefits are denoted by 0% since this case is used as the basis for comparison. The data in columns 3–7 are for vehicle strings 2–6, respectively. For the fuel and emission data, a positive number means improvement while a negative number means deterioration. The notation "≈ 0" in the table represents benefits between -4% and 4% and is considered to be negligible due to inaccuracies in the emission model. Due to the aggressive response of the manual truck, the fuel and emission benefits are minor except for NO_x. The smooth response of the ACC trucks filters the disturbance created by the lead vehicle, presenting a smoother speed response to be tracked by the passenger vehicles following the truck. As a result, some benefits with respect to fuel and emissions are shown in Table I. These benefits are small due to the fact that the disturbance created was a rather smooth one (low acceleration). In this case, the travel time is not affected.

We also evaluate the fuel consumption and emission results for heavy trucks in these simulations and the data are presented in Table II. The ACC trucks lead to better fuel consumption and emission results compared to the manually driven truck. However, there is little difference among the four different ACC trucks. The benefits are small, however, due to a low level of disturbance.

TABLE III
TRAVEL TIME, FUEL, AND EMISSION BENEFITS OF THE EIGHT PASSENGER VEHICLES FOLLOWING THE TRUCK IN A STRING OF TEN VEHICLES FOR HIGH-ACCELERATION MANEUVERS OF THE LEAD VEHICLE (NO CUT-INS)

Vehicle String (with)	1 (M_PV)	2 (M_T)	3 (ACC_N)	4 (ACC_Q)	5 (ACC_C)	6 (ACC_NEW)
Travel Time(sec)	96.0	96.2	95.4	95.3	95.4	95.4
Fuel (g)	0% (1020)	15.5%	21.5%	22.7%	22.4%	23.8%
CO (g)	0% (251.2)	87.9%	89.4%	89.9%	89.9%	90.2%
HC (g)	0% (4.02)	65.1%	68.4%	71.5%	71.4%	73.1%
NO_x (g)	0% (4.21)	52.1%	56.0%	60.6%	60.3%	67.6%

TABLE IV
FUEL AND EMISSION BENEFITS OF THE HEAVY TRUCKS IN HIGH-ACCELERATION MANEUVERS (NO CUT-INS)

	M_T	ACC_N	ACC_Q	ACC_C	ACC_NEW
Fuel (g)	0% (802.0)	10.6%	12.7%	12.6%	12.6%
CO (g)	0% (7.09)	9.2%	11.1%	11.0%	11.2%
HC (g)	0% (0.34)	4.4%	5.2%	5.1%	5.2%
NO_x (g)	0% (18.14)	7.6%	9.5%	9.5%	10.5%

TABLE V
TRAVEL TIME, FUEL, AND EMISSION BENEFITS OF THE EIGHT PASSENGER VEHICLES FOLLOWING THE TRUCK IN A STRING OF TEN VEHICLES FOR HIGH-ACCELERATION MANEUVERS WITH OSCILLATIONS OF THE LEAD VEHICLE (NO CUT-INS)

Vehicle String (with)	1 (M_PV)	2 (M_T)	3 (ACC_N)	4 (ACC_Q)	5 (ACC_C)	6 (ACC_NEW)
Travel Time(sec)	96.0	96.2	95.4	95.3	95.4	95.4
Fuel (g)	88.0	88.1	87.5	87.5	87.6	87.6
CO (g)	0% (860.3)	23.9%	29.7%	34.2%	34.0%	36.1%
HC (g)	0% (298.3)	90.2%	93.5%	94.5%	94.5%	94.9%
NO_x (g)	0% (4.45)	73.7%	79.3%	82.4%	82.8%	84.1%

TABLE VI
FUEL AND EMISSION BENEFITS OF THE TRUCKS IN HIGH-ACCELERATION MANEUVERS WITH OSCILLATIONS (NO CUT-INS)

	M_T	ACC_N	ACC_Q	ACC_C	ACC_NEW
Fuel (g)	0% (618.2)	12.0%	23.1%	22.9%	27.4%
CO (g)	0% (5.55)	10.6%	20.0%	20.0%	23.8%
HC (g)	0% (0.28)	4.8%	8.5%	8.5%	12.4%
NO_x (g)	0% (13.2)	9.1%	17.0%	17.2%	21.6%

B. High-Acceleration Maneuvers

In this case, the lead passenger vehicle accelerates from 8 to 20 m/s with a constant acceleration of 2.0 m/s^2 and then cruises at a constant speed. As in test 1, we consider the same six strings of vehicles with ten vehicles in each string. The travel time is recorded over a distance of 1.7 km as this is the distance taken by the vehicles to reach a steady-state speed after completing the acceleration maneuver.

Table III shows the travel time and fuel consumption and emission results for the last eight passenger vehicles in the simulations with high-acceleration maneuvers. The presence of heavy trucks little affects the travel times, but significantly increases the fuel efficiency and decreases emissions of the following passenger vehicles. The trucks act as lowpass filters presenting a much smoother speed response to be tracked by the vehicles following the trucks in the string. Furthermore, it is observed that all the ACC trucks lead to better fuel consumption and emissions compared with the manual truck. The new ACC system has the best improvements. Table IV shows the fuel consumption and emission results for different trucks. All the ACC trucks have better results in terms of fuel efficiency and emissions compared with the manually driven truck. However, there is little difference among the four different ACC trucks.

C. High-Acceleration Maneuvers With Oscillations

The purpose of this test is to examine the effect of the truck (second in the string) on the behavior of the following eight passenger cars when the lead vehicle performs a high-acceleration oscillatory maneuver creating a disturbance that propagates upstream. The lead passenger vehicle accelerates from 8 to 16 m/s with a constant acceleration of 2.0 m/s^2, and its speed oscillates around 16 m/s before settling to the constant speed of 16 m/s. The travel time is recorded over a distance of 1.3 km as this is the distance taken by the vehicles to reach a steady-state speed after completing the acceleration maneuver.

Table V shows the fuel consumption and emission results for the last eight passenger vehicles in each vehicle string. It follows from Table V that the presence of heavy trucks can significantly improve the fuel efficiency and decrease most of the emissions. This is due to the fact that the inherent sluggish characteristics of the heavy trucks can attenuate the high-frequency components in the speed of the lead vehicle. Among the ACC trucks, ACC_NEW leads to the best results in all aspects, since it filters the oscillations in the lead vehicle's speed more effectively than the others. Again, we can observe the travel times are little affected by the heavy trucks. Table VI shows the fuel consumption and emissions results for different trucks. All the ACC trucks lead to better fuel consumption and emissions results compared with the manually driven truck, and the performance of the new ACC system is the best.

D. Speed-Limit Effect

In the previous simulations, we assume that the lead vehicle reaches a steady state giving time for the truck to close in by using a higher speed leading to a travel time that is not affected by the presence of the truck. However, if the lead vehicle reaches a speed that the truck cannot exceed due to load or speed limits, the travel time will be affected. In the simulations, we consider two vehicle strings used in the previous simulations: string 1 (all manually driven passenger vehicles) and string 6 (with ACC_NEW in the second position). The lead passenger vehicle accelerates from 8 to 24 m/s with a constant acceleration of 1.0 m/s^2, and then cruises at a constant speed. Here, we assume the speed limit is 24 m/s. In string 1, all the following passenger vehicles respond similarly to those shown in Fig. 2(a), and the data are not presented here. The speed and separation error responses in string 6 are shown in Fig. 5. ACC_NEW increases its speed sluggishly and the separation error keeps increasing until its speed reaches the limit. As marked in Fig. 5(b), at the

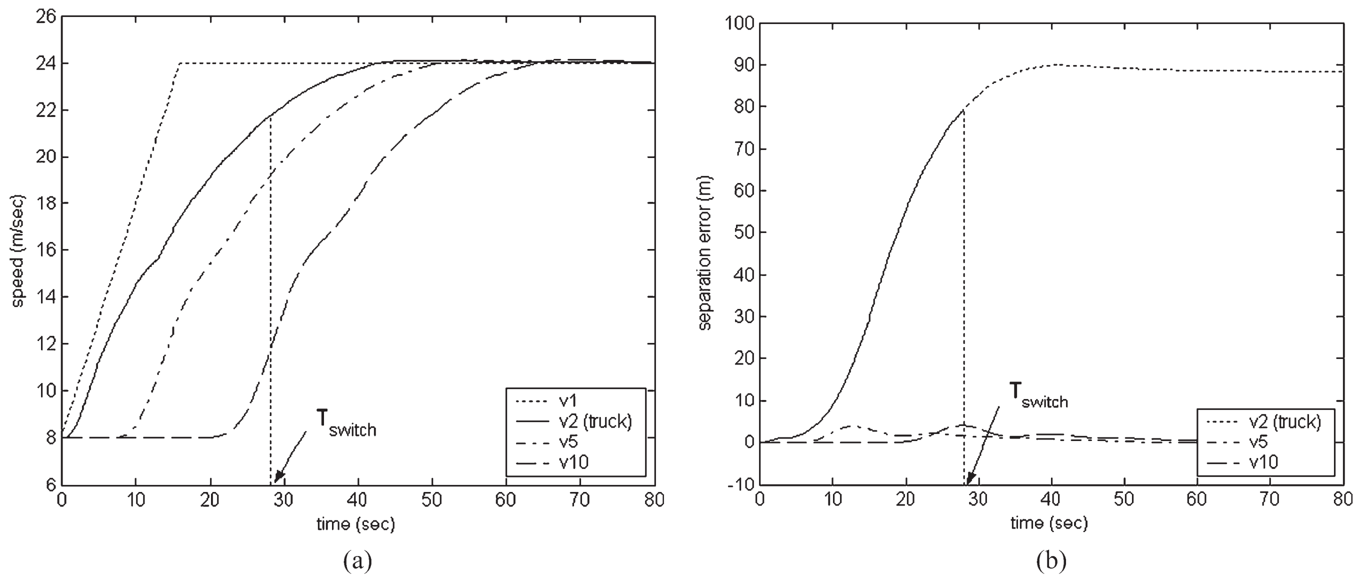

Fig. 5. Speed-limit effect. (a) Speed responses and (b) separation error responses of the vehicles in string 6 (the second vehicle is an ACC truck with the new controller).

TABLE VII
TRAVEL TIME, FUEL, AND EMISSION DATA OF THE EIGHT PASSENGER VEHICLES IN STRINGS 1 AND 6 IN THE SIMULATIONS WITH SPEED LIMIT (NO CUT-INS)

Vehicle String	M_PV in the 2nd position	ACC_NEW in the 2nd position
Travel Time (sec)	68.8	71.7
Fuel (g)	774	691 (10.7%)
CO (g)	77.6	24.2 (68.8%)
HC (g)	1.84	1.06 (42.4%)
NO_x (g)	3.01	1.48 (50.8%)

time T_{switch}, the intervehicle distance becomes larger than the maximum operating range of the ranging sensor and the ACC controller switches from the vehicle-following mode to the speed tracking mode. The separation error response is plotted with dotted line after T_{switch} since the ranging sensor no longer provides any separation signal. We consider the travel time, fuel consumption, and emissions for the last eight passenger vehicles after they have traveled 1.3 km and present them in Table VII. As we can see, though the presence of ACC_NEW significantly decreases the fuel consumption and emissions, the travel time has been increased (by about 2.9 s).

E. Lane-Change Effect

The motivation for studying lane-change effects in mixed traffic with heavy trucks and passenger vehicles is based mostly on the fact that the sluggish response of the heavy truck results in a large temporary gap between the truck and the accelerating passenger vehicle in front, giving rise to multiple cut-ins from the neighboring lanes. The truck is considered to be equipped with the new ACC system, followed by eight passenger vehicles. We consider the situation where the passenger vehicle leading the ACC truck accelerates from 8 to 20 m/s with a constant acceleration of 2 m/s^2 and then cruises with a constant speed creating a large intervehicle spacing. In the simulations, it is assumed that when the spacing between the truck and its preceding vehicle is large enough (larger than $s_0 + 2.8v_{\mathrm{t}}$, where v_{t} is the truck speed), one or more passenger vehicles from the neighboring lane cut in between the two vehicles and position themselves with safe intervehicle spacings. In the simulations, three vehicles cut in at 5, 10.6, and 17.5 s, respectively, and with the speeds of 12.2, 18.0, and 21.0 m/s, respectively. These cut-ins are shown in Fig. 6. We consider the travel time, fuel consumption, and emissions for the last eight passenger vehicles after they have traveled 1.7 km and present them in the right column of Table VIII. For comparison purposes, the corresponding data for the situation without cut-in vehicles are also presented in Table VIII. From Table VIII, we can see that the disturbance created by the cut-ins has a small negative effect on fuel consumption and emissions, and the travel time is increased by about 4 s due to the cut-ins.

It is shown that the presence of heavy trucks in the mixed traffic can significantly improve fuel consumption and emissions of the passenger vehicles in the presence of disturbances due to high-acceleration maneuvers. The heavy trucks act as filters present to the following vehicles smoother speed responses to be tracked. Furthermore, the ACC trucks lead to better fuel and emissions results than the manually driven trucks due to their smoother responses. The newly developed ACC controller provides the best performance among all the ACC controllers, and it filters the oscillations more effectively in the case of high-acceleration maneuvers with oscillations.

In such situations, another effect takes place as the sluggish response of the truck creates large intervehicle gaps inviting vehicles from neighboring lanes to cut in front of the truck. This effect depends on cut-in situations considered. If we consider aggressive cut-ins, for example, a passenger vehicle at a low-speed cuts in just a few meters ahead of the heavy truck, forcing the truck to decelerate and then speed up, the disturbance created in such scenario may have a more adverse effect on fuel economy and pollution. Furthermore, cut-ins will create

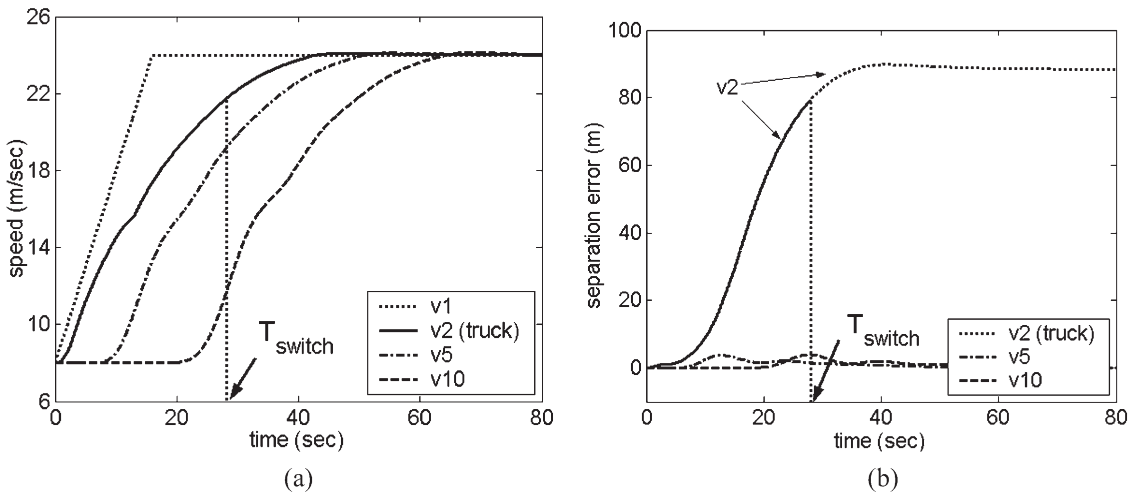

Fig. 6. Lane-change effect. (a) Speed responses and (b) separation error responses of the vehicles in string 6 (the second vehicle is an ACC truck with the new controller).

TABLE VIII
TRAVEL TIME, FUEL, AND EMISSION DATA OF THE EIGHT PASSENGER VEHICLES FOLLOWING ACC_NEW IN HIGH-ACCELERATION MANEUVERS, WITHOUT CUT-IN(S) AND WITH THREE CUT-INS

	Without Cut-in(s)	With Cut-in(s)
Travel Time (sec)	95.4	99.5
Fuel (g)	776	811 (-4.5%)
CO_2 (g)	2418	2531 (-4.7%)
CO (g)	24.2	24.3 (-0.4%)
HC (g)	1.08	1.11 (-2.8%)
NO_x (g)	1.36	1.40 (-2.9%)

disturbances in the neighboring lane too with adverse effects on fuel economy and pollution for the vehicles in those lanes. Our conclusion is that while the heavy trucks with or without ACC have smooth responses and filter traffic disturbances, their sluggish behavior will create large gaps, inviting cut-ins, which may take away any benefits their filtering response will have for the vehicles in their lane. Furthermore, the cut-ins will create additional disturbances in the neighboring lanes that will also have a negative effect on fuel economy and pollution. The travel time of the vehicle following after heavy trucks may be affected by the speed limits or cut-in vehicles.

VI. Experimental Validation

Experiments with three actual vehicles were conducted at Crows Landing test field to validate the simulation models and designed controllers. The lead vehicle was a Buick LeSabre with an automatic speed tracking system. The second vehicle was the heavy truck (about 15 T) with different ACC systems. The lidar system installed on the truck was used as the ranging sensor providing separation distance and relative speed between the preceding vehicle and the truck. The controllers used in the simulation section were used in the experiments. The third vehicle was a manually driven Buick LeSabre, following the truck as in normal traffic.

The experiments demonstrated that all the ACC controllers work on an actual truck in a vehicle-following environment [16]. We simulate the same scenarios as in the experiments using our simulation models. In particular, we consider a string of three vehicles where the first vehicle is made to generate the same speed trajectories as in the experiments, the second one is a heavy truck with one of the designed controllers, and the third one is modeled using Pipes' model. Here, we only present one set of experiment and simulation data to demonstrate the validation of the simulation results, and more data can be found in [16]. In the validation test, the first vehicle generates one speed trajectory that was used in the experiments, which is plotted with the red dotted line in Fig. 7(a), labeled as "first vehicle." The speed responses of the ACC truck (with the constant-time-headway policy) and the passenger vehicle are plotted in Fig. 7(a) with broken lines and labeled as "second vehicle (ACC truck), simulation" and "third vehicle (Pipes' model), simulation," respectively. The corresponding experimental data are also plotted in Fig. 7(a) with solid lines and labeled as "second vehicle (ACC truck), experiment" and "third vehicle, experiment," respectively. The engine-torque responses in the simulation and experiment are plotted in Fig. 7(b). The simulation results are very close to the experiment results. Additional validation tests supported the same conclusion: The designed vehicle-following controller works on actual trucks, and the nonlinear model used for heavy trucks and Pipes' model used to model human-driver response in the longitudinal direction are valid for studying vehicle following in a mixed traffic situation. Consequently, our simulation models and results can be used with confidence in studying vehicle-following characteristics and effects involving more vehicles in a mixed traffic situation.

VII. Conclusion

In this paper, we design, analyze, and evaluate the performance of a PID-type vehicle-following controllers with different spacing policies. A new vehicle-following controller is designed to provide better performance, which is demonstrated by simulations and emission analysis. Experiments involving actual vehicles are used to validate our simulation models, at least on the microscopic level, and demonstrate that the proposed vehicle-following controllers work in real time and under actual driving conditions.

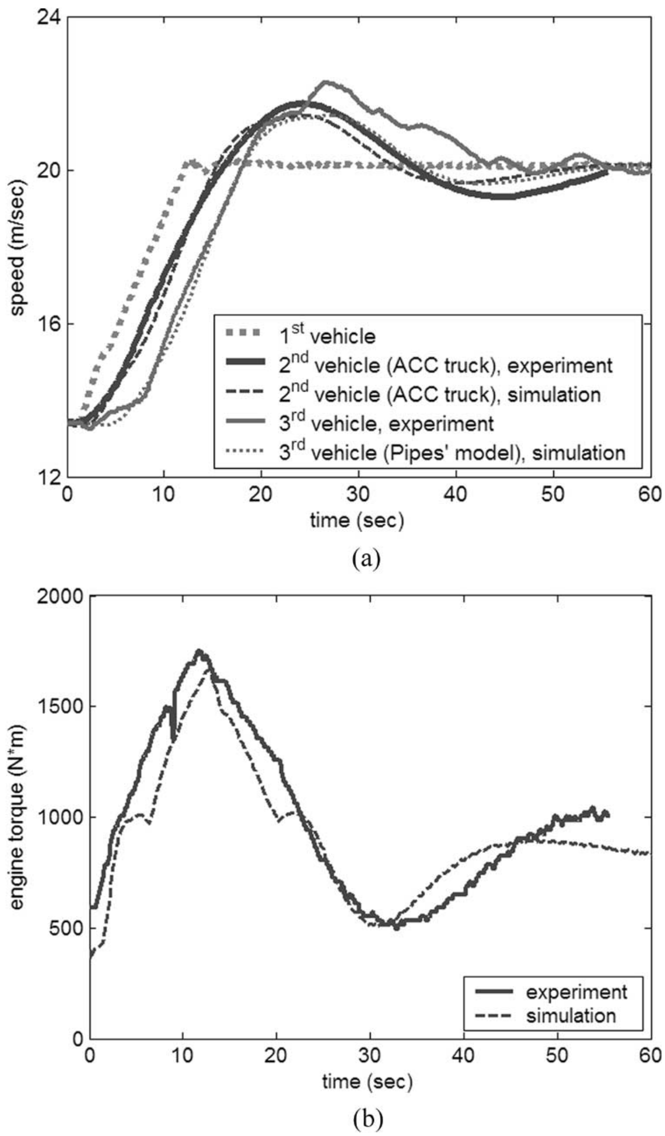

Fig. 7. Experimental testing. (a) Speed responses of the three vehicles (the second is ACC_C) and (b) engine-torque responses of ACC_C in the experiment and simulation.

The sluggish dynamics of trucks, whether manual or ACC, due to limited acceleration and speed capabilities, make their response to disturbances caused by lead passenger vehicles smooth. The vehicles following the truck are therefore presented with a smoother speed trajectory to track. This filtering effect of trucks is shown to have beneficial effects on fuel economy and pollution. The quantity of the fuel and emission benefits depends very much on the level of the disturbance and scenario of maneuvers. If the response of the truck is too sluggish relative to the speed of the lead vehicle, then a large intervehicle spacing may be created, inviting cut-ins from neighboring lanes. These cut-ins create additional disturbances with negative effects on fuel economy and pollution. Situations can be easily constructed where the benefits obtained due to the filtering effect of trucks are eliminated due to disturbances caused by possible cut-ins. Furthermore, cut-ins are shown to increase travel time for the vehicles in the original traffic stream.

Acknowledgment

The contents of this paper reflect the views of the authors who are responsible for the facts and the accuracy of the data presented herein. The contents do not necessarily reflect the official views or policies of the State of California. This paper does not constitute a standard, specification, or regulation.

References

[1] J. G. Parker, "Trucks in a row," *Traffic World*, vol. 259, no. 2, p. 23, Jul. 12, 1999.

[2] T. Kelly, "Keeping trucks on track," *ITS World*, vol. 99, no. 4, pp. 20–21, Jul./Aug. 1999.

[3] D. Yanakiev and I. Kanellakopoulos, "Longitudinal control of automated CHVs with significant actuator delays," *IEEE Trans. Veh. Technol.*, vol. 50, no. 5, pp. 1289–1297, Sep. 2001.

[4] ——, "Nonlinear spacing policies for automated heavy-duty vehicles," *IEEE Trans. Veh. Technol.*, vol. 47, no. 4, pp. 1365–1377, Nov. 1998.

[5] ——, "Analysis, design, and evaluation of AVCS for heavy-duty vehicles: Phase 1 report," California PATH Program, Inst. Transp. Studies, Univ. California, Berkeley, California PATH Research Rep. UCB-ITS-PWP-95-12, 1995.

[6] ——, "Engine and transmission modeling for heavy-duty vehicles," California PATH Program, Inst. Transp. Studies, Univ. California, Berkeley, California PATH Research Rep., Tech Note 95-06, 1995.

[7] A. Bose and P. Ioannou, "Analysis of traffic flow with mixed manual and semiautomated vehicles," *IEEE Trans. Intell. Transp. Syst.*, vol. 4, no. 4, pp. 173–188, Dec. 2003.

[8] P. Ioannou and M. Stefanovic, "Evaluation of ACC vehicles in mixed traffic: Lane change effects and sensitivity analysis," *IEEE Trans. Intell. Transp. Syst.*, vol. 6, no. 1, pp. 79–89, Mar. 2005.

[9] S. C. Jolibois and A. Kanafani, "An assessment of IVHS-APTS technology impacts on energy consumption and vehicle emissions of transit bus fleets," California PATH Program, Inst. Transp. Studies, Univ. California, Berkeley, California PATH Research Rep. UCB-ITS-PRR-94-19, 1994.

[10] M. Barth, T. Younglove, and G. Scora, "Development of a heavy-duty diesel modal emissions and fuel consumption model," in *Proc. 12th Coordinating Research Council On-Road Emissions Workshop*, San Diego, CA, PATH Rep. UCB-ITS-PRR-2005-01, Apr. 2002.

[11] M. J. Barth *et al.*, *User's Guide: Comprehensive Modal Emissions Model, version 2.0*. Riverside, CA: Univ. California Press, 2000.

[12] L. A. Pipes, "An operational analysis of traffic dynamics," *J. Appl. Phys.*, vol. 24, no. 3, pp. 271–281, 1953.

[13] M. Bando, K. Hasebe, A. Nakayama, A. Shibata, and Y. Sugiyama, "Dynamical model of traffic congestion and numerical simulation," *Phys. Rev. E, Stat. Phys. Plasmas Fluids Relat. Interdiscip. Top.*, vol. 51, no. 2, pp. 1035–1042, Feb. 1995.

[14] A. Mason and A. Woods, "Car-following model of multi-species systems of road traffic," *Phys. Rev. E, Stat. Phys. Plasmas Fluids Relat. Interdiscip. Top.*, vol. 55, no. 3, pp. 2203–2214, Mar. 1997.

[15] P. Ioannou and T. Xu, "Throttle and brake control systems for automatic vehicle following," *IVHS J.*, vol. 1, no. 4, pp. 345–377, 1994.

[16] J. Zhang and P. Ioannou, "Control of heavy-duty trucks: Environmental and fuel economy considerations," California PATH Program, Inst. Transp. Studies, Univ. California, Berkeley, California PATH Research Rep. UCB-ITS-PRR-2004-15, 2004.

[17] K. Yi, S. Lee, and Y. D. Kwon, "An investigation of intelligent cruise control laws for passenger vehicles," *Proc. Inst. Mech. Eng. D, Automob. Eng.*, vol. 215, no. 2, pp. 159–169, Feb. 2001.

[18] F. Broqua, G. Lerner, V. Mauro, and E. Morello, "Cooperative driving: Basic concepts and a first assessment of intelligent cruise control strategies," in *Proc. DRIVE Conf. Advanced Telematics Road Guidance*, Brussels, Belgium, Feb. 4–9, 1991, pp. 908–929.

[19] D. Swaroop and R. Huandra, "Intelligent cruise control systems and traffic flow stability," *Transp. Res.,* vol. 7, no. 6, part C, pp. 329–352, Dec. 1999.

[20] P. Ioannou and J. Sun, *Robust Adaptive Control*. Englewood Cliffs, NJ: Prentice-Hall, 1996.

[21] J. Zhang and P. Ioannou. (Oct. 2005). "Adaptive cruise control design for heavy trucks and its environmental impacts," Reseach Lab. CATT, University of Southern California, LA, USC Rep. No. 1. [Online]. Available: www-rcf.usc.edu/~ioannou/reports

[22] H. S. Bae and J. C. Gerdes, "Command modification using input shaping for automated highway systems with heavy trucks," in *Proc. Amer. Control Conf.*, Denver, CO, 2003, vol. 1, pp. 54–59.

Jianlong Zhang (S'04–M'06) received the B.S. degree from the University of Science and Technology of China, Hefei, China, in 1999 and the M.S. degree from the Vanderbilt University, Nashville, TN, in 2001. He is currently working toward the Ph.D. degree with the Department of Electrical Engineering—Systems, University of Southern California, Los Angeles.

His research interests include nonlinear and adaptive control, intelligent transportation systems, and modeling and control of mechatronic and pneumatic systems.

Mr. Zhang received the University President Award from the University of Science and Technology of China in 1998.

Petros A. Ioannou (S'80–M'83–SM'89–F'94) received the B.Sc. degree in mechanical engineering with "first class honors" from the University College London, London, U.K., in 1978 and the M.S. in mechanical engineering and Ph.D. degrees in electrical engineering from the University of Illinois, Urbana, in 1980 and 1982, respectively.

In 1982, he joined the Department of Electrical Engineering—Systems, University of Southern California, Los Angeles. He is currently a Professor in the same department and the Director of the Center of Advanced Transportation Technologies. He also holds a joint appointment with the Department of Aerospace and Mechanical Engineering. He is the author/coauthor of five books and over 150 research papers in the area of controls, neural networks, nonlinear dynamical systems, and intelligent transportation systems. His research interests are in the areas of adaptive control, neural networks, nonlinear systems, vehicle dynamics and control, intelligent transportation systems, and marine transportation.

Dr. Ioannou was a recipient of the Outstanding Transactions Paper Award from IEEE Control Systems Society and the recipient of a 1985 Presidential Young Investigator Award for his research in Adaptive Control in 1984. He has been an Associate Editor for the IEEE TRANSACTIONS ON AUTOMATIC CONTROL, the *International Journal of Control*, *Automatica*, and IEEE TRANSACTIONS ON INTELLIGENT TRANSPORTATION SYSTEMS. He also served as a member of the Control System society on IEEE Intelligent Transportation Systems (ITS) Council Committee, and his center on advanced transportation technologies was a founding member of Intelligent Vehicle Highway System (IVHS) America, which was later renamed ITS America. He is currently an Associate Editor at Large of the IEEE TRANSACTIONS ON AUTOMATIC CONTROL and a Chairman of the International Federation of Automatic Control (IFAC) Technical Committee on Transportation Systems.